A Hybrid Diesel-Wind-PV-Based Energy Generation System with Brushless Generators

B.Jeshwardhan Raj & M.Madhusudhan Reddy

[1]PG scholar Department of Electrical and Electronics Engineering
[2]Assoc.Professor Department of Electrical and Electronics Engineering
Dr.K.V.Subba Reddy Institute of Technology

Abstract—

This paper presents an experimental implementation of a standalone micro grid topology based on a single voltage source converter (VSC) and brushless generators. The micro grid system is energized with different renewable energy sources namely wind and solar PV array. However, a diesel generator (DG) set and a battery energy storage system (BESS) are also used to maintain the reliability of the system. The proposed topology has the advantage of reduced switching devices and simple control. The implemented topology has DG set as an ac source. The wind generator and the solar PV array are dc sources which are connected to the dc link of the VSC. The BESS is also used at the dc link to facilitate the instantaneous power balance under dynamic conditions. Along with the system integration, the VSC also has the capability to mitigate the power quality problems such as harmonic currents, load balancing, and voltage regulation. A wide variety of test results are presented to demonstrate all the features of the proposed system.

Index:- Terms—Brushless generator, composite observer, power quality, standalone micro grid, voltage regulation, voltage source converter (VSC).

I.INTRODUCTION

THERE are many locations in the world where the small localities are developed far away from the well-developed societies. It is technically and economically difficult to setup a transmission system to make electricity available there due to the cost incurred, the problems related to grounding of the transmission tower at hilly areas and Right of Way problems due to forests in between. However, on the other hand, these areas have abundance of natural resources like solar energy, wind, hydro, etc. Due to the uncertain nature of all these renewable energy sources, a small self-sustaining supply system cannot be established which can supply the loads continuously. To make the system self-sustaining, some reliable sources are required. Therefore, generally a diesel generator (DG) is used at these sites. To account for randomness of the natural resources, a full rating DG is a costly option. Some energy storage device can be employed there, which reduces the DG rating and considerable fuel consumption.

As described earlier, since the system is setup at a remote area, the brushless generators [1] are used to avoid the maintenance as much as possible. The

proposed topology in this paper includes solar PV array and wind energy as natural resources. A sub- stantial literature is available for different topologies, control, operational aspects, power electronics of the wind, and solar PV systems [2]–[5]. Authors have proposed many topologies, con- trol algorithms and operation strategies for the micro grid system with many energy sources. Like doubly fed induction genera- tors are used for the wind- and diesel-based system [6], where the controller is optimizing the fuel consumption and regulating the voltage and frequency of the system with maximum avail- able power extraction from wind. Different operating strategies to include wind power in a diesel-based system to save fuel and to reduce the overall cost of the system are proposed in [7] and [8]. A time frame-based control algorithm is proposed in [9] for a wind-diesel system with an energy storage. In this paper, authors have proposed an energy storage system to account for wind randomness and fuel cost. A standalone hybrid wind-solar system with an engine generator and a battery is proposed in [10], where the operational aspects and topology are described. The proposed topology has six VSCs to integrate the complete system. Lin et al. [11] have proposed a solar and diesel–wind hybrid generation system with BESS, in which a synchronous generator is used for a diesel generator which requires automatic voltage regulator (AVR) and speed governor for voltage and frequency regulation. Yogianto et al. [12] have proposed different configurations of a hybrid system using solar PV array, wind,

and diesel systems. An optimal operation of solar PV/diesel hybrid system without storage is described in [13]. With the given load profile of an area for whole day, size and scheduling of the generator are performed to maximize the generator efficiency. Similarly to reduce the battery size and to increase efficiency of the system, an ultra-capacitor is used with the battery to ex- change power during dynamics and the battery is used to supply under sustained load generator power mismatch [14]. Along with these different topologies and control strategies, other studies are also reported in the literature. Simulation studies are carried out for a micro grid system with many sources and energy storage devices with different controllers to regulate the frequency of the system [15]. Different generators are used with the diesel engine and the studies are performed with diesel, PV, and diesel- PV mixed generation. Moreover, the short circuit studies are performed on the system by Bonino et al. [16]. Reliability evaluation of a wind-diesel-battery-based system is reported by Xu et al. [17], where wind energy conversion system reliability is obtained taking into consideration the wind fluctuations and component failure. Moreover, the reliability analysis of the complete system is also performed by taking diesel, wind, and battery.

The control of a permanent magnet synchronous generator (PMSG) based wind energy conversion system (WECS) connected to an inverter with battery acting as a grid is presented in [18]. The power

generated by WECS is used to control the SOC of battery. In most of the systems, described in the literature, variable speed wind energy conversion system operates to extract the maximum power from the wind. Wind energy is free energy at the operation stage, so it is beneficial to extract the maximum power and to increase the efficiency and the utilization of WECS. It needs initial capital cost, but the fuel is free. There are many topologies and algorithms reported for MPPT in WECS and solar PV system. As in [19]–[21], different methods for MPPT in WECS are proposed like algorithm similar to hill climbing, the mechanical sensor less MPPT algorithm with the current controlled inverter, and the mechanical sensor less MPPT algorithm with a boost converter. Basic MPPT algorithms for solar PV system are described in [22] and [23]. These are per- turb and observe algorithm and incremental conductance-based algorithm.

Moreover, a control algorithm is required to control the VSC connected for its operation as voltage and frequency controller, mitigating power quality problems and integrating the dc sources with ac sources. Many basic control algorithms are reported in the literature. Singh and Solanki [24] have reported SRF, IRPT, and ADALINE based control algorithms and Icos phi based algorithm for DSTATCOM [25]. An advanced control algorithm based on composite observer is reported in [26]. Composite observers are used to extract harmonic components from any signal and

then the extracted fundamental is further used in this control algorithm [27], [28].

This paper deals with an implementation of a reduced converter topology of a diesel-wind-solar PV-based standalone micro grid system with the BESS. These generators are synchronous reluctance generator (SyRG) and permanent magnet brushless dc generator (PMBLDCG). Both these generators are brushless in construction. The wind and solar PV systems are always operated at their maximum power point using boost converters and the DG is operated within a specified power range to optimize the efficiency of the DG. A VSC is used to integrate the DC sources with the AC sources with the bidirectional power flow capability and the power quality improvement capability. A mechanical sensor less MPPT algorithm is used for WECS and an incremental conductance based MPPT algorithm is used for solar PV system.
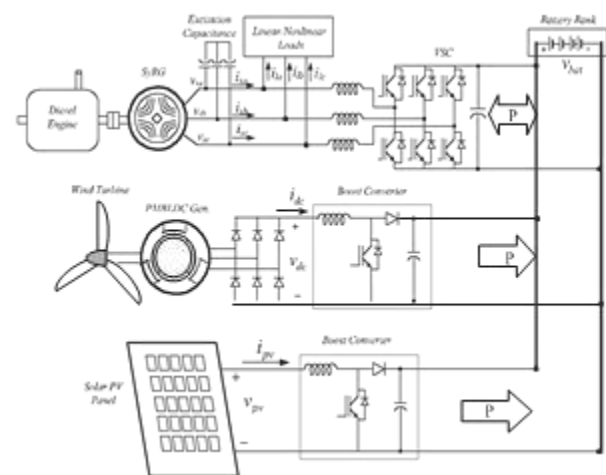

Fig.1.Proposed single VSC and the brushless generation-based standalone micro grid system.

II. STANDALONE MICROGRID TOPOLOGY

The proposed system is a diesel-wind-so6lar PV based standalone micro grid with the battery energy storage to feed the local loads. The complete system topology is shown in Fig. 1. A SyRG is used as a DG and a PMBLDCG as a wind generator. These generators are selected purposefully due to the following reasons. Both these generators are brushless generators that reduce the maintenance cost relative to the brushed ones. For a DG, SyRG is used rather than a conventional synchronous generator, so the need of a speed governor and AVR is eliminated yet the voltage and frequency of the system are regulated using VSC. The PMBLDC generator is driven by a wind turbine. As shown in Fig. 1, the WECS is connected at the dc link of the VSC through a diode rectifier and a boost converter. PMBLDCG is best suited for an uncontrolled rectification due to trapezoidal back EMF. If the winding currents are also made quasi-square wave, then a low-ripple torque is produced and the machine operates smoothly. This feature is not there with PMSG as the EMF generated is sinusoidal, so the quasi-square wave currents produce a fluctuating torque. Moreover, the energy density of the PMBLDC machine is high which makes it small in size, hence good option for pole mounting application. The proposed topology also includes solar PV system, which is also connected to the dc link of the VSC for power transfer to the ac side where loads are present. As discussed earlier, to maintain the power balance and reliability of the supply, the battery energy storage device is required. Hence, a battery bank is also installed at the dc link of the VSC.

III. CONTROL STRATEGY FOR PROPOSED STANDALONE MICROGRID SYSTEM

The proposed system topology has many sources, so an operational strategy is developed to optimize the fue6l efficiency and to maximize the extraction of free energy available. The DG is the only ac source in the system, so the system and the load end frequency is related to the operation of the DG only. A constant frequency of the system means the constant speed of the generator (as the generator is SyRG). It is stated in [29] that with fixed speed operation of the diesel engine, the fuel consumption does not vary much from its value at full load, thus making the diesel engine fuel efficiency poor at lighter loads. The diesel engines operate at reasonable good efficiency between 80–100% loading. Here, the control strategy is developed for the DG to operate it always within a specified loading range as shown in Fig. 2. The DG with rating as full load rating is not required as there are renewable energy resources and the battery energy storage device is available.

The WECS consists of a PMBLDC generator, three-phase diode bridge rectifier (DBR) and a boost converter. An inductor is used after the DBR to make the dc current almost constant which reflects as quasi-square waveform of current on the ac side which is beneficial for the operation of PMBLDCG as discussed earlier. The operation of the WECS is simplified by eliminating the need of any mechanical sensor for MPPT. An MPPT algorithm is

used which requires only sensing of *v*dc and *i*dc. This MPPT algorithm is the same as perturb and observe, which is used for maximum power extraction in solar PV system.

III. CONTROL STRATEGY FOR PROPOSED STANDALONE MICROGRID SYSTEM

The proposed system topology has many sources, so an operational strategy is developed to optimize the fuel efficiency and to maximize the extraction of free energy available. The DG is the only ac source in the system, so the system and the load end frequency is related operation of the DG only.

making the diesel engine fuel efficiency poor at lighter loads. The diesel engines operate at reasonable good efficiency between 80–100% loading. Here, the control strategy is developed for the DG to operate it always within a specified loading range as shown in Fig. 2.

The DG with rating as full load rating is not required as there are renewable energy resources and the battery energy storage device is available.
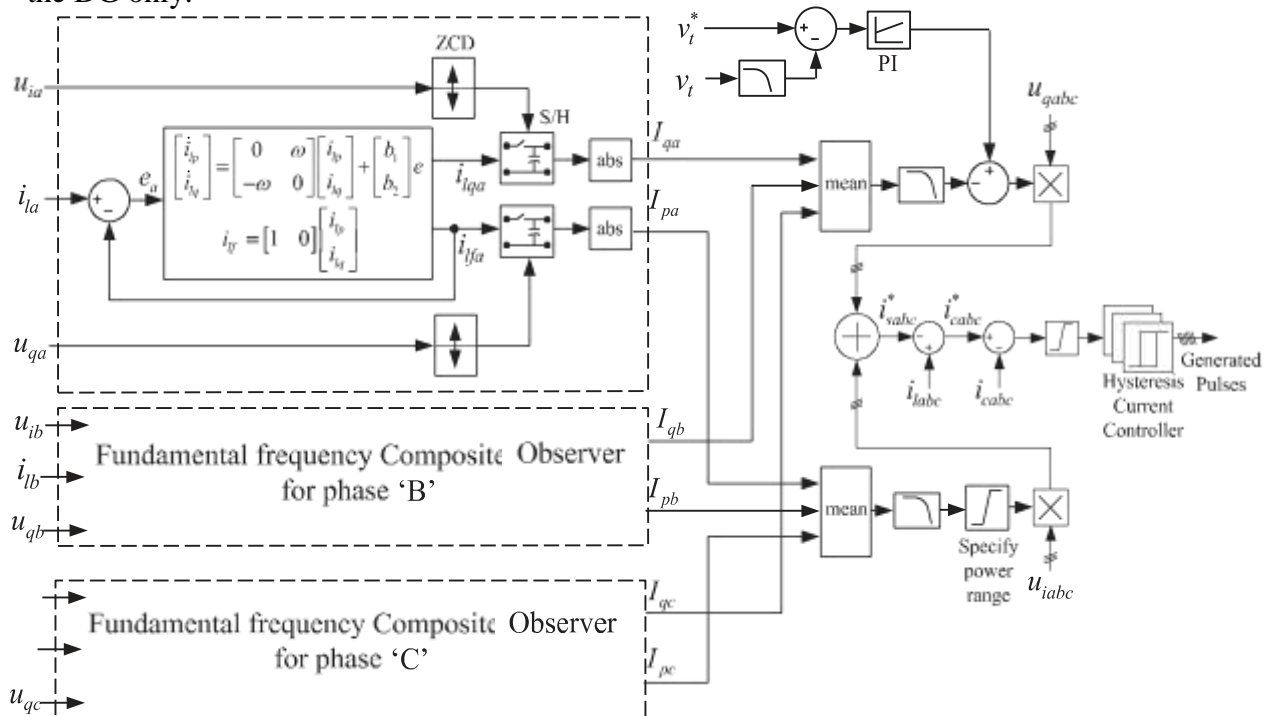

Fig. 2. Control strategy for VSC.

A constant frequency of the system means the constant speed of the generator (as the generator is SyRG). It is stated in [29] that with fixed speed operation of the diesel engine, the fuel consumption does not vary much from its value at full load, thus

The WECS consists of a PMBLDC generator, three-phase diode bridge rectifier (DBR) and a boost converter. An inductor is used after the DBR to make the dc current almost constant which reflects as quasi-square waveform of current on the ac side which is beneficial for the operation of

PMBLDCG as discussed earlier. The operation of the WECS is simplified by eliminating the need of any mechanical sensor for MPPT. An MPPT algorithm is used which requires only sensing of *v*dc and *i*dc. This MPPT algorithm is the same as perturb and observe, which is used for maximum power extraction in solar PV system.

A. Voltage and Frequency Control of DG

Any distorted signal like voltage or current can be decomposed in to the dc and different frequencies sinusoidal signals as defined by Fourier series. All these frequency components can be estimated online using composite observers. However, the control algorithm for this system requires only fundamental frequency component estimation. So a composite observer is used to extract the fundamental frequency component of the load currents. The basic structure of a composite observer is described here. It creates a specified frequency in-phase and quadrature-phase components of the input signal. The state space representation of one unit of composite observer is shown as

$$\dot{X}n = \Omega_n X_n + B_n\ e; \quad y_n = C_n\ X_n\ ;$$
where *n* = harmonic order

$$\dot{X}_n = [\ \dot{X}_{1n}\quad \dot{X}_{2n}\ ]^T, X_n = [X_{1n}\ X_{2n}]^T$$

$$\Omega_n = \begin{bmatrix} 0 & n\omega \\ -n\omega & 0 \end{bmatrix}, B_n = \begin{bmatrix} b_{1n} \\ b_{2n} \end{bmatrix}, C_n = \begin{bmatrix} 1 \\ 0 \end{bmatrix}. \quad (1)$$

As described in (1), with a composite observer having many units present for different harmonics, each unit tends to extract the particular harmonic component for which it is tuned. Thus, combination of all these components converges towards the actual signal. So in this type of system, the error "e" eventually becomes zero.

However, with the proposed scheme, only unit corresponding to the fundamental frequency is used, which extracts only fundamental frequency component. The in-phase component of load current is obtained as output of the system and the quadrature-phase is obtained as the internal state of the system.

The characteristic of a unit of the composite observer corresponding to $\omega = 2\pi/50$ rad/s can be derived.

The transfer function of (3b) is similar to a peak filter and with the selected value of *b*1 and *b*2 , the quality can be adjusted. Using these in-phase and quadrature-phase components of load currents, the active and reactive power components of the load currents are estimated as shown in Fig. 2. For generation of reference source currents, in-phase and quadrature-phase unit vectors of PCC voltage are required. Their calculation is described in [25].

The control algorithm for the VSC to act as voltage and frequency controller is shown in Fig. 2.VSC maintains the active power output of the generator thereby regulating the frequency indirectly and it provides reactive power required to maintain the voltage.

B. Mechanical Sensor less-Based MPPT Algorithm for WECS

The wind energy is free energy as there is no fuel cost, so WECS is operated to extract the maximum available power from the wind. An MPPT algorithm is used to perform this task. To simplify the control and to make it cost effective, an MPPT algorithm is used which does not require measurement of any of wind speed, rotor speed, or turbine speed [21]. Hence,

mechanical speed sensor is eliminated by virtue of the proposed system configuration and control algorithm. A perturb and observe-based MPPT algorithm is used to control the boost converter which extracts the maximum power from the wind generator. The mathematical formulation for MPPT algorithm is described as

where $p\mathrm{dc} = v\mathrm{dc}.i\mathrm{dc}$ and δ is a small value. The $i$ref and $i$dc are reference and sensed inductor current of the boost converter.

The current is perturbed by a small value (δ) and the power output is observed for the change. In case, the power increases, the next perturbation is kept in the same direction to force the system toward MPP. However, in case the power decreases, the direction of perturbation is changed to pull back the system toward the MPP. The duty cycle is used to generate pulse width modulation pulses as shown in Fig. 3.
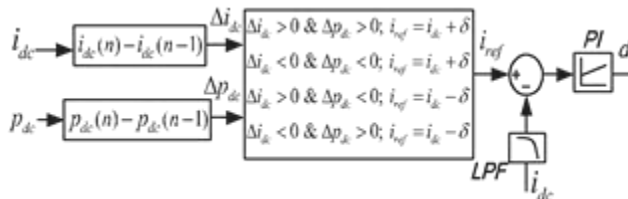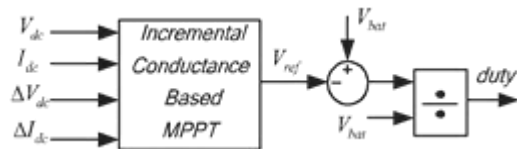

Fig. 3. Control system for WECS.

Fig. 4. Control system for solar PV system.

C. Incremental Conductance-Based MPPT Algorithm for Solar PV System

The maximum power available from a solar PV array is extracted using an incremental conductance-based algorithm [23].This MPPT algorithm gives the reference voltage of the PV array at which it

should be operated to provide maximum power output. The reference duty ratio for the boost converter switch is estimated using reference PV array voltage and the known battery voltage. The corresponding gate pulse for the boost converter switch is generated as shown in Fig. 4.

D. Charge Discharge Control of Battery Storage

As the focus of the paper is on the hybrid generation system, the battery charge discharge control is not considered much. But this section is dedicated to provide some idea behind power flows in the topology and how battery status can be monitored and controlled. On a large scale, the power flow between the various sources can be demonstrated as in Fig. 5. It can be seen that other than battery, all the other currents/powers are measured. So it would not be difficult to estimate the battery current and take actions accordingly. With the described topology and controls, the battery charge discharge can be controlled usingthe available control of each power source and load as shown in Fig. 5.
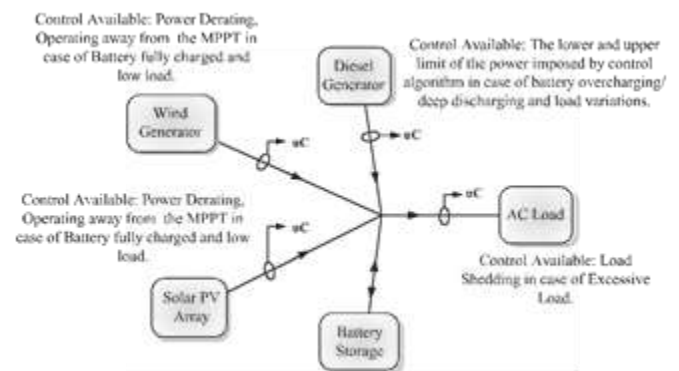

Fig. 5. Power flow and available controls in the system.

If some situation arises where the charge discharge has to be exactly monitored, a current sensor can be installed in the system to measure the battery current. The battery

voltage is already being measured and these can be used to determine the state of charge and other parameters to control charge discharge.
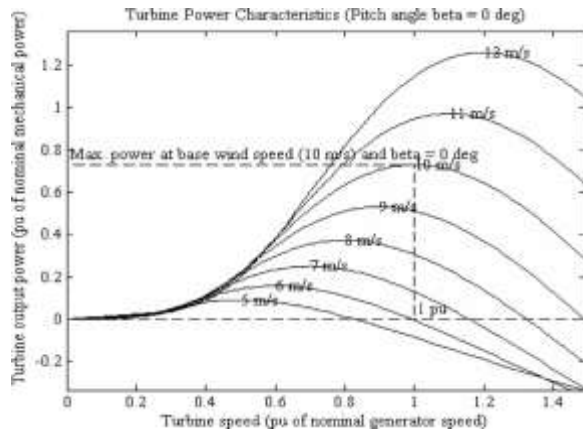

Fig. 6. Wind turbine characteristics for different wind speeds.

IV. EXPERIMENTAL RESULTS AND DISCUSSION

An experimental prototype of the proposed micro grid system described earlier is developed in the laboratory and the control algorithm and the operation strategy are verified on this system. The system information is provided in Appendix. The DG is operated under specified power range. The wind and solar systems are operated always at MPP. The MPPT algorithm for the wind has not been tested on the experimental system due to the unavailability of the wind turbine emulation facility. The MPPT algorithm is verified using simulation and the experimentation is performed for verifying the control considering that the reference current $i$dc to be tracked is available.

A. Steady State and Dynamic Performance of Simulation-Based Verification of MPPT Algorithm for WECS

As described earlier, the complete system is simulated using MATLAB/SIMULINK and from simulation results the MPPT of WECS is verified. A basic wind turbine model is considered for this purpose [30]. The power characteristic of the simulated wind turbine is shown in Fig. 6. The pitch angle is taken as fixed and the base wind speed as 10 m/s. The corresponding performance of the MPPT algorithm under variable wind operation is shown in Fig. 7. The results with constant wind speed are shown in Fig. 7 until t=4 s. The wind speed is changed from 10 to 12 m/s at t = 4 s. The dynamic behavior of the system is demonstrated during such variation in wind speed. From these results, it is seen that with an increase in the wind speed, the power output of the WECS increases and also it can be seen that the PMBLDCG current has also increased.
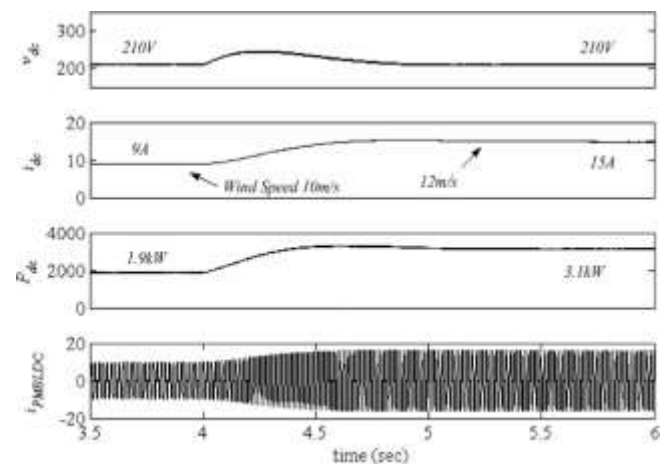

Fig. 7. Performance of WECS under varying wind speed.

B. Steady-State Performance of Standalone System

The proposed system is operated under various loading conditions to verify

the control algorithm. The loading conditions are defined according to the state of the battery whether charging or discharging. Steady-state results of the system in both the conditions are shown in Figs. 8 and 10. Fig. 8(a)–(c) show the three-phase source currents ($i$sabc) and Fig. 8(d)–(f) show the load currents ($i$labc). From here, it can be seen that in addition to voltage and frequency control, the VSC is also performing the task of harmonics elimination, load balancing, and reactive power compensation. All three source currents are almost balanced and sinusoidal. The VSC currents ($i$cabc) shown in Fig. 8(g)–(i) verify this compensation. Fig. 8(j), (k) show the PMBLDC generator current (iPMBLDCG) and the dc side current of DBR ($i$dc). The PMBLDCG current (iPMBLDCG) is approximately a quasi-square wave current and the $i$dc confirms that the WECS system is working well and the power is extracted from the PMBLDCG.

Fig. 8(l) shows the battery current. As the load is almost fed by the DG, the energies coming from the solar PV array and the WECS are stored in the battery. Fig. 8(m), (n) show the PV voltage and current and the battery voltage and boost converter output current. Fig. 8(o) shows the power extracted from the PV system. Fig. 9 confirms that the power extracted from the PV array is the maximum power that could be extracted under given condition. It can be seen that both the power readings are almost the same and the MPP scale shows that power from the PV system is tracked at almost 99.7% of the MPP value. Fig. 8(p), (q) show the harmonic content of the source and load currents. The power quality improvement capability of the VSC along with the voltage and frequency control is demonstrated. The THD of source current is only 4.9%, thereby negligible harmonic

currents are entering the machine windings, hence no extra losses and thus no derating of the machine is required. The voltage THD is shown in Fig. 8(r). This shows the quality of supply given to the customer loads.

The performance of the microgrid system under heavily loaded condition is shown in Fig. 10. Fig. 10(a) shows the source current ($i$sa) and Fig. 10(b) shows the load current ($i$la), which are significantly more than the source currents. Even the system is heavily loaded, the DG is still supplying the load with in the specified power range. Fig. 10(c) shows the VSC current ($i$ca).PMBLDC generator current (iPMBLDCG) is shown in Fig. 10(d). The power output from the WECS is kept the same for the comparison purpose. With the same power from the wind turbine and solar PVarray, if the system loading is increased, the DG hits its upper power limit and the load is then fed from the battery. This is seen from Fig. 10(e) where the battery current is negative and hence the battery is discharging. This confirms the functioning of the control strategy for the complete system. Fig. 10(f) shows the battery voltage and the output current of the boost converter after solar array, $i$pvo.. In this case also, the solar PV current and voltage which are the same as previous case of light load. It can be seen from Fig. 10(f), $i$pvo,that the power obtained from solar PV array is kept the same as in previous case.
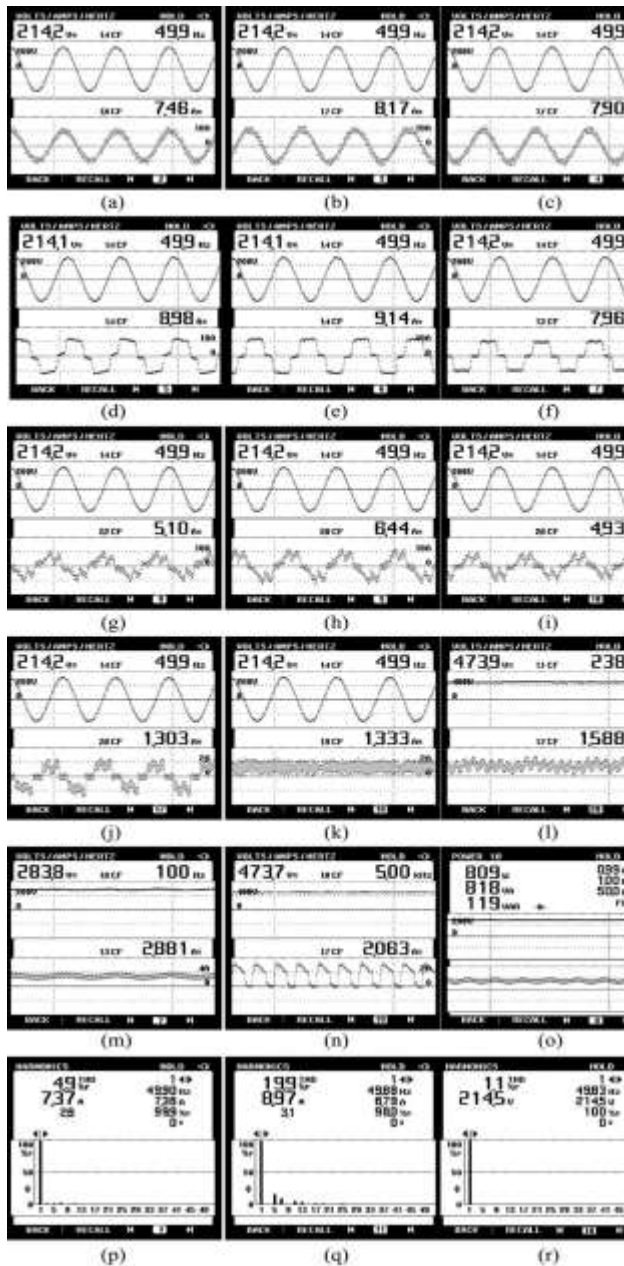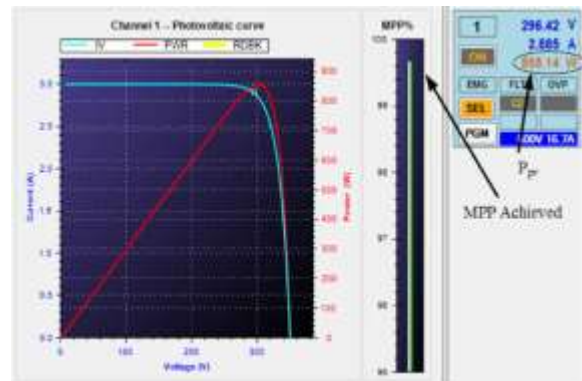
Fig. 9. User interface of solar emulator showing Ppv and ipv versus vpv , performance of MPPT algorithm.

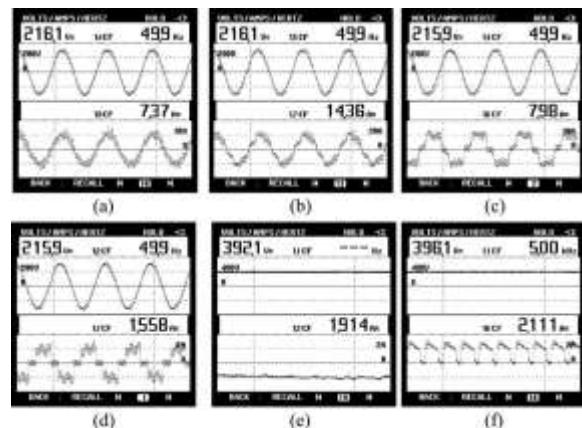*Fig. 10. Steady-state performance under heavy load condition (a) Vab, Isa ; (b) Vab, ila ; (c) Vab, Ica ;*

(d) Vab , iPMBLDCG ; (e) Vbat, Ibat ; and (f)Vbat, ipvo

C. Dynamic Performance of the Proposed Microgrid System

The proposed system topology along with the associated control algorithm is tested for the performance of the controllers under various disturbances and the randomness of the renewable energy resources. The response of the system is verified for sudden load changes like removing load on one phase. Fig. 11(a) shows that even after removing the load of phase a, the source current remains unchanged and the voltage of the system is also constant. This drastically reduces the load on the system and also creates a large

Fig. 8. Steady-state performance under light load condition, (a)–(c) vab , isabc ; (d)–(f) vab, ilabc ; (g)–(i) vab, icabc ; (j) vab , iPMBLDCG ; (k) vab, idc; (l) vbat, ibat ; (m) vpv, ipv ; (n) vbat, ipvo ; (o) Ppv ; (p) harmonic content of isa ; (q) harmonic content of ila ; and (r) harmonic content of vab .

unbalanced load. The performance is checked in terms of the capability of the system to survive with this sudden load rejection and injection. Moreover, the controller is designed to maintain the balanced source currents.
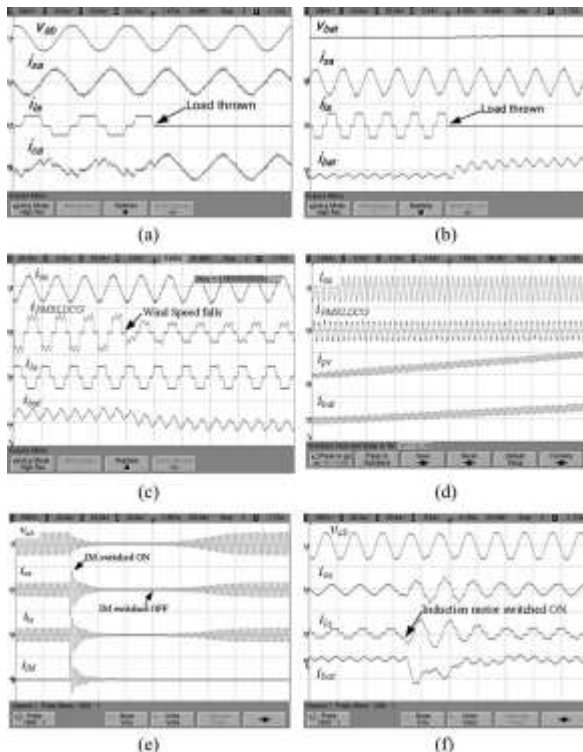

Fig. 11. Dynamic performance (a) vab, isa, ila and ica; (b) vbat, isa , ila and ibat; (c) isa, iPMBLDCG, ila and ibat; (d) isa, iPMBLDCG , ipv and ibat; (e) vab, isa, ila and iIM ; and (f) vab, isa, iLa and ibat .

The system is stable under load variations and also the source currents are balanced and maintained as per the control. Fig. 11(b) shows that with load removal, the extra power goes to the battery, so the battery is going from discharging mode to charging mode. The WECS is also tested for variable speed or change in power reference. It is shown in Fig. 11(c) that keeping the load unchanged, with a decrease in wind speed, the battery starts discharging to feed the load. So the deficiency created due to wind speed fall is fulfilled by the battery as

it can be seen that the battery current is becoming negative (discharging mode).

Other renewable source is solar PV energy, so it is also uncertain in nature. So with change of the insolation level, the power output of the solar PV array changes. The effect of this change is shown in Fig. 11(d). Maintaining the power from WECS constant, with an increase in solar insolation, the battery starts charging by the extra power.
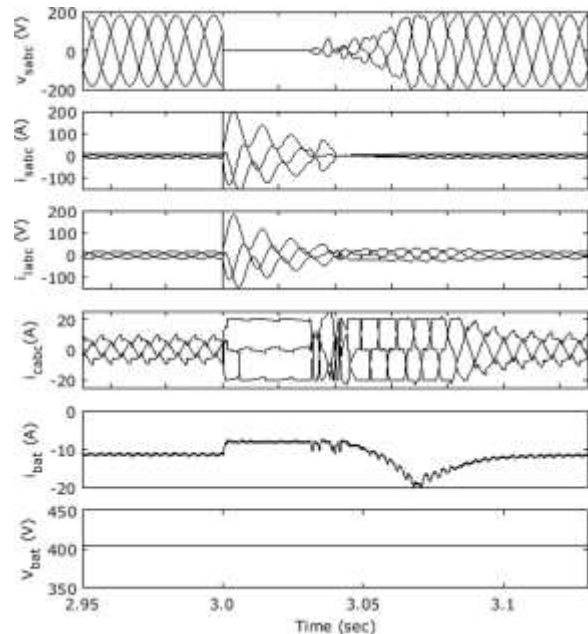

Fig. 12. System performance under faulted condition.

The operation of system is validated under an induction motor load. As the starting current of an induction motor is high, so a system has to be reasonably stable and well controlled to feed such type of dynamic loads. Fig. 11(e) shows the response of the system without any control or no voltage and frequency regulation. It can be seen that with the induction motor starting, the voltage of the system collapses and on removing the motor the voltage regains. So this system cannot survive without a proper controller. On

incorporating the complete system with voltage and frequency controller, the performance can be seen in Fig. 11(f). The system voltage is effectively maintained constant and the starting transient is taken care by the battery.

D. System Performance Under Faulted Condition

This section provides a brief understanding of how the system will behave under some fault conditions. The fault situations are created and analyzed using simulation tool. First case is taken where the fault is created at the ac bus. Current through the converter is controlled within the control algorithm. As the currents are non-sinusoidal, a hard current limit is used to protect the devices and the system. If the switching devices have their own protection system (like desaturation for IGBTs), then an indirect current control can be used, which requires only source currents. But those protections are latch able (shutdown the system), so it is better to limit the current without disrupting the operation. That is why a direct current control incorporating compensator currents is used. The results are shown in Fig. 12. As shown in Fig. 12, the reactive power support to the generator is mostly provided by the converter and with the fault on the ac line, the reactive power diverts to the low-impedance fault path and the generator's voltage collapses. But as soon as the fault is cleared, the generator picks up again. Another advantage of this system is that it is a machine-based system and hence the generator majorly contributes to the fault current, which has a large short circuit rating compared to the semiconductor devices. Moreover, the fault current in such cases is large, which makes the protection system design easier. Other case could be fault at the dc bus, which is catastrophic in every

case of energy storage. In that case, the battery will be protected by the fuse or MCB and the system has to shut down. Or in some cases, the storage can be isolated and the load can be fed by generator, but that can be achieved only by observing the load conditions and maintaining power balance, e.g., shedding load in case of overload. In that case, the converter can act as a shunt compensator to provide reactive power support.

V. CONCLUSION

The proposed micro grid topology with a single voltage source converter and brushless generators has been implemented under various operating conditions. An integrated operation of control algorithms is also tested for system's voltage and frequency control, mitigation of power quality issues, power balance in the whole system under various disturbances ranging from large load variation to renewable energy supply uncertainty. Some idea of battery charge discharge control and fault analysis is also discussed. Test results have confirmed the suitability of this topology for rural/isolated areas as the topology is simple and cost effective.

APPENDIX

A. SyRG Rating: three-phase, 3.7 kW, 230V, 1500 r/min, 22.7A, 50 Hz.
B. PV Array Rating: Open Circuit Voltage = 350 V (at1000 W/m2 and 25 °C), short circuit current = 3 A.
C. Battery Rating: 400 V, 2.8 kWh.
D. Controller: dSPACE 1104 R&D Controller.

REFERENCES

[1] L. L. Lai and T. F. Chan, Distributed Generation—Induction and Permanent Magnet Generators. Hoboken, NJ, USA: Wiley, 2007.

[2] B.Wu, Y. Lang, N. Zargari, and S. Kouro, Power Conversion and Control of Wind Energy Systems. Hoboken, NJ, USA: Wiley, 2011.

[3] S. C. W. Krauter, Solar Electric Power Generation— Photovoltaic Energy Systems: Modeling of Optical and Thermal Performance, Electrical Yield, Energy Balance, Effect on Reduction of Greenhouse Gas Emissions. New York, NY, USA: Springer, 2007.

[4] P. Nema, R. K. Nema, and S. Rangnekar, "A current and future state of art development of hybrid energy system using wind and PV-solar: Areview," J. Renew. Sustain. Energy Rev., vol. 13, no. 8, pp. 2096–2103, Oct. 2009.

[5] J. M. Carrasco et al., "Power-Electronic systems for the grid integration of renewable energy sources: A survey," IEEE Trans. Ind. Electron., vol. 53, no. 4, pp. 1002–1016, Jun. 2006.

[6] R. Pena, R. Cardenas, J. Proboste, J. Clare, and G. Asher, "Wind–Diesel generation using doubly fed induction machines," IEEE Trans. Energy Convers., vol. 23, no. 1, pp. 202–214, Mar. 2008.

[7] D. G. Infield, G.W. Slack, N. H. Lipman, and P. J. Musgrove, "Review of wind/diesel strategies," IEE Proc. A—Phys. Sci.,Meas. Instrum., Manage. Educ.—Rev., vol. 130, no. 9, pp. 613–619, Dec. 1983.

[8] R. Sebastian and R. Pena-Alzola, "Study and simulation of a battery based energy storage system for wind diesel hybrid systems," in Proc. IEEE Int. Energy Conf. Exhib., Sep. 2012, pp. 563–568.

[9] C. Abbey, Li Wei, and G. Joos, "An online control algorithm for application of a hybrid ESS to a wind–diesel system," IEEE Trans. Ind. Electron., vol. 57, no. 12, pp. 3896–3904, Dec. 2010.

[10] T. Hirose and H.Matsuo, "Standalone hybrid wind-solar power generation system applying dump power control without dump load," IEEE Trans. Ind. Electron., vol. 59, no. 2, pp. 988–997, Feb. 2012.

[11] W.-M. Lin, C.-M. Hong, and C.-H. Chen, "Neural-network-based MPPT control of a stand-alone hybrid power generation system," IEEE Trans. Power Electron., vol. 26, no. 12, pp. 3571–3581, Dec. 2011.

[12] A. Yogianto, H. Budiono, and I. A. Aditya, "Configuration hybrid solar system (PV), wind turbine, and diesel," in Proc. Int. Conf. Power Eng. Renew. Energy, Jul. 2012, pp. 1–5.

[13] D. Yamegueu, Y. Azoumah, X. Py, and N. Zongo, "Experimental study of electricity generation by solar PV/diesel hybrid systems without battery storage for off-grid areas," J. Renewable Energy, vol. 36, no. 6, pp. 1780–1787, Jun. 2011.

[14] M. A. Tankari, M. B. Camara, B. Dakyo, and G. Lefebvre, "Use of ultra-capacitors and batteries for efficient energy management in wind–diesel hybrid system," IEEE Trans. Sustain. Energy, vol. 4, no. 2, pp. 414–424, Apr. 2013.

[15] D. C. Das, A. K. Roy, and N. Sinha, "GA based frequency controller for solar thermal— diesel—wind hybrid energy generation/energy storage system," Int. J. Electr. Power Energy Syst., vol. 43, no. 1, pp. 262–279, Dec. 2012.

[16] F. Bonanno, A. Consoli, A. Raciti, B. Morgana, and U. Nocera, "Transient analysis of integrated diesel-wind-photovoltaic generation systems," IEEE Trans. Energy Convers., vol. 14, no. 2, pp. 232–238, Jun. 1999.

[17] L. Xu, S. Islam,A.A.Chowdhury, and D.O.Koval, "Reliability evaluation of a wind-diesel-battery hybrid power system," in Proc. IEEE/IAS Ind. Commercial Power Syst. Tech. Conf., May 2008, pp. 1–8.

[18] J. De Matos, F. E. Silva, and L. Ribeiro, "Power control in AC isolated micro grids with renewable energy sources and energy storage systems," IEEE Trans. Ind. Electron., vol. 62, no. 6, pp. 3490–3498, Jun. 2015.

[19] R-J Wai, C. Y. Lin, and Y. R. Chang, "Novel maximum-power-extraction algorithm for PMSG wind generation system," IET Elect. Power Appl., vol. 1, no. 2, pp. 275–283, Mar. 2007.

[20] K. Tan and S. Islam, "Optimum control strategies in energy conversion of PMSG wind turbine system without mechanical sensors," IEEE Trans. Energy Convers., vol. 19, no. 2, pp. 392–399, Jun. 2004.

[21] Z. M. Dalala, Z. U. Zahid, W. Yu, Y. Cho, and J.-S. Lai, "Design and analysis of an MPPT technique for small-scale wind energy conversion systems," IEEE Trans. Energy Convers., vol. 28, no. 3, pp. 756–767, Sep. 2013.

[22] D. Sera, L. Mathe, T. Kerekes, S. V. Spataru, and R. Teodorescu, "On the perturb-and-observe and incremental conductance MPPT methods for PV systems," IEEE J. Photovolt., vol. 3, no. 3, pp. 1070–1078, Jul. 2013.

[23] M. A. Elgendy, B. Zahawi, and D. J. Atkinson, "Assessment of the incremental conductance maximum power point tracking algorithm," IEEE Trans. Sustain. Energy, vol. 4, no. 1, pp. 108–117, Jan. 2013.

[24] B. Singh and J. Solanki, "A comparison of control algorithms for DSTATCOM," IEEE Trans. Ind. Electron., vol. 56, no. 7, pp. 2738–2745, Jul. 2009.

[25] B. Singh and S. Kumar, "Control of DSTATCOM using IcosΦ algorithm," in Proc. 35th Annu. Conf. IEEE Ind. Electron., Nov. 2009, pp. 322–327.

[26] B. Singh and S. R. Arya, "Composite observer-based control algorithm for distribution static compensator in four-wire supply system," IET Power Electron., vol. 6, no. 2, pp. 251–260, Feb. 2013.

[27] K. Selvajyothi and P. A. Janakiraman, "Extraction of harmonics using composite observers," IEEE Trans. Power Del., vol. 23, no. 1, pp. 31–40, Jan. 2008.

[28] K. Selvajyothi and P. A. Janakiraman, "Analysis and simulation of single phase composite observer for harmonics extraction," in Proc. Int. Conf. Power Electron. Drives Energy Syst., Dec. 2006, pp. 1–6.

[29] A. K. Jain, V. T. Ranganathan, V. K. Kumar, and G. Guruswamy, "Diesel engine driven stand-alone variable speed constant frequency slip ring induction generator - theory and experimental results," in Proc. Nat. Power Electron. Conf., IIT Roorkee, Roorkee, India, Jun. 2010.

[30] H. Siegfried, Grid Integration of Wind Energy Conversion Systems. Hoboken, NJ, USA: Wiley, 1998.